UC Berkeley

Title
First results of the plasma wakefield acceleration experiment at PITZ

Permalink

Authors
Lishilin, O
Gross, M
Brinkmann, R
et al.

Publication Date

DOI

Peer reviewed

First results of the plasma wakefield acceleration experiment at PITZ

O. Lishilin [a,*], M. Gross [a], R. Brinkmann [b], J. Engel [a], F. Grüner [c,d], G. Koss [a], M. Krasilnikov [a], A. Martinez de la Ossa [b], T. Mehrling [b], J. Osterhoff [b], G. Pathak [a], S. Philipp [a], Y. Renier [a], D. Richter [e], C. Schroeder [f], R. Schütze [a], F. Stephan [a]

[a] Deutsches Elektronen-Synchrotron, DESY, Zeuthen, Germany
[b] Deutsches Elektronen-Synchrotron, DESY, Hamburg, Germany
[c] Universität Hamburg, UHH, Hamburg, Germany
[d] Center for Free-Electron Laser Science, CFEL, Hamburg, Germany
[e] Helmholtz-Zentrum Berlin, HZB, Berlin, Germany
[f] Lawrence Berkeley National Laboratory, LBNL, Berkeley, USA

ARTICLE INFO

ABSTRACT

The self-modulation instability of long particle beams was proposed as a new mechanism to produce driver beams for proton driven plasma wakefield acceleration (PWFA). The PWFA experiment at the Photo Injector Test facility at DESY, Zeuthen site (PITZ) was launched to experimentally demonstrate and study the self-modulation of long electron beams in plasma. Key aspects for the experiment are the very flexible photo-cathode laser system, a plasma cell and well-developed beam diagnostics. In this contribution we report about the plasma cell design, preparatory experiments and the results of the first PWFA experiment at PITZ.

© 2016 Elsevier B.V. All rights reserved.

1. Introduction

The Advanced Wakefield Experiment (AWAKE) is launched at CERN to demonstrate and study the proton driven plasma wakefield acceleration [1,2]. The parameters of the accelerated electrons depend strongly on the wake exited by a proton bunch. One of the key aspects of the upcoming experiment is the period of the wakefields which are triggered by the self-modulation instability of long proton bunches. To maximize the accelerating field, the proton bunch length has to be roughly equal to the inverse plasma wavenumber, $\sigma_z = \frac{\lambda_p}{\sqrt{2}\pi}$ [3]; however these parameters for proton beams are not available at currently existing hadron accelerators. It was shown that by propagation in plasma the long bunch excites a plasma wave [4] and then the plasma wave splits the beam into short bunches. The period of the resulting bunch structure is about the plasma wave length [5,6]. Since the physical processes for protons and electrons are very similar [7], it was proposed to use the Photo Injector Test facility at DESY, Zeuthen site (PITZ) for demonstrating and studying of the self-modulation mechanism of long electron bunches in plasma. PITZ offers a unique photoinjector laser system and extensive beam diagnostics, including a transverse deflecting cavity and a high resolution electron spectrometer.

2. PITZ photocathode laser and diagnostics

The photocathode laser for PITZ was developed and built by the Max Born Institute, Berlin. Key element of the laser system is a pulse shaper [8], a set of 13 motorized birefringent crystals which allows to transform an initial short Gaussian pulse (about 2 ps FWHM) to a flat top temporal profile with short rise and fall times, defined by the length of the initial pulse, and up to 24 ps FWHM pulse length. The main diagnostic device to be used in the self-modulation experiment is an S-band travelling wave transverse deflecting structure (TDS). Commissioning of this device, which enables the recording of the longitudinal phase space of the electron beam after passing the plasma when operated together with an electron spectrometer, started in 2015 [9]. The simulated longitudinal resolution with ideal beam transport is about 100 μm, while the modulation period of 1 mm is defined by the plasma wavelength to get several modulation periods along the beam. The simulated energy modulation in the experiment is about 400 keV, and the simulated resolution of the energy measurement using TDS and HEDA2 dipole spectrometer with ideal beam transport is 10 keV. Screen stations downstream the plasma cell can also be used for the observation of self-modulation signatures (beam size, beam core to beam halo ratio).

3. Simulation of the PITZ experiment

An initial feasibility of the self-modulation experiment at PITZ was indicated with a start-to-end simulation including the

---

full particle-in-cell (PIC) code OSIRIS [10], while a fine tuning of beam parameters was done with the quasi-static PIC code HiPACE [11,12]. The particle tracking code ASTRA [13] was used to track the beam from the photo-electron gun to the entrance of the plasma and from the plasma exit to the diagnostics downstream the plasma cell. A sinusoidal signature of the self-modulation instability is seen at the longitudinal phase space after the plasma cell (Fig. 1(b)), the electron beam is split into several sub-bunches with a length of about the plasma wavelength. The transport to the electron spectrometer was optimized with ASTRA (Fig. 1(c)). Further on, the measurement of the longitudinal phase space was simulated, with the result shown in Fig. 1(d). Although the signature is washed out compared to the situation directly after the TDS, the self-modulation of the beam can be seen clearly, showing that the resolution of the PITZ setup is suitable to measure the self-modulation of the electron beam.

4. Plasma cell construction

The plasma cell design is defined by two factors: requirements of the plasma volume (density, length, sharpness of edges) and space restrictions in the PITZ beamline. The basic design is based on the SLAC plasma source [14]. The plasma cell is a cross-shaped heat pipe oven (Fig. 2) where lithium is heated and evaporated in the center of the cell. The vapor is condensed at the cooled ends of the pipe and the liquid metal is transported back to the center by means of a capillary force in a metal mesh which covers the inner surface of the pipe. The lithium vapor density is constant and defined by the buffer gas pressure at a given temperature. At the ends of the pipe two thin foils are mounted. Their function is to separate the plasma cell atmosphere from the beam line vacuum. The windows have to be thick enough to prevent gas permeation and withstand pressure differences, but at the same time the thickness should be minimal to prevent electron beam scattering. An ArF laser is used to ionize the lithium vapor with the laser
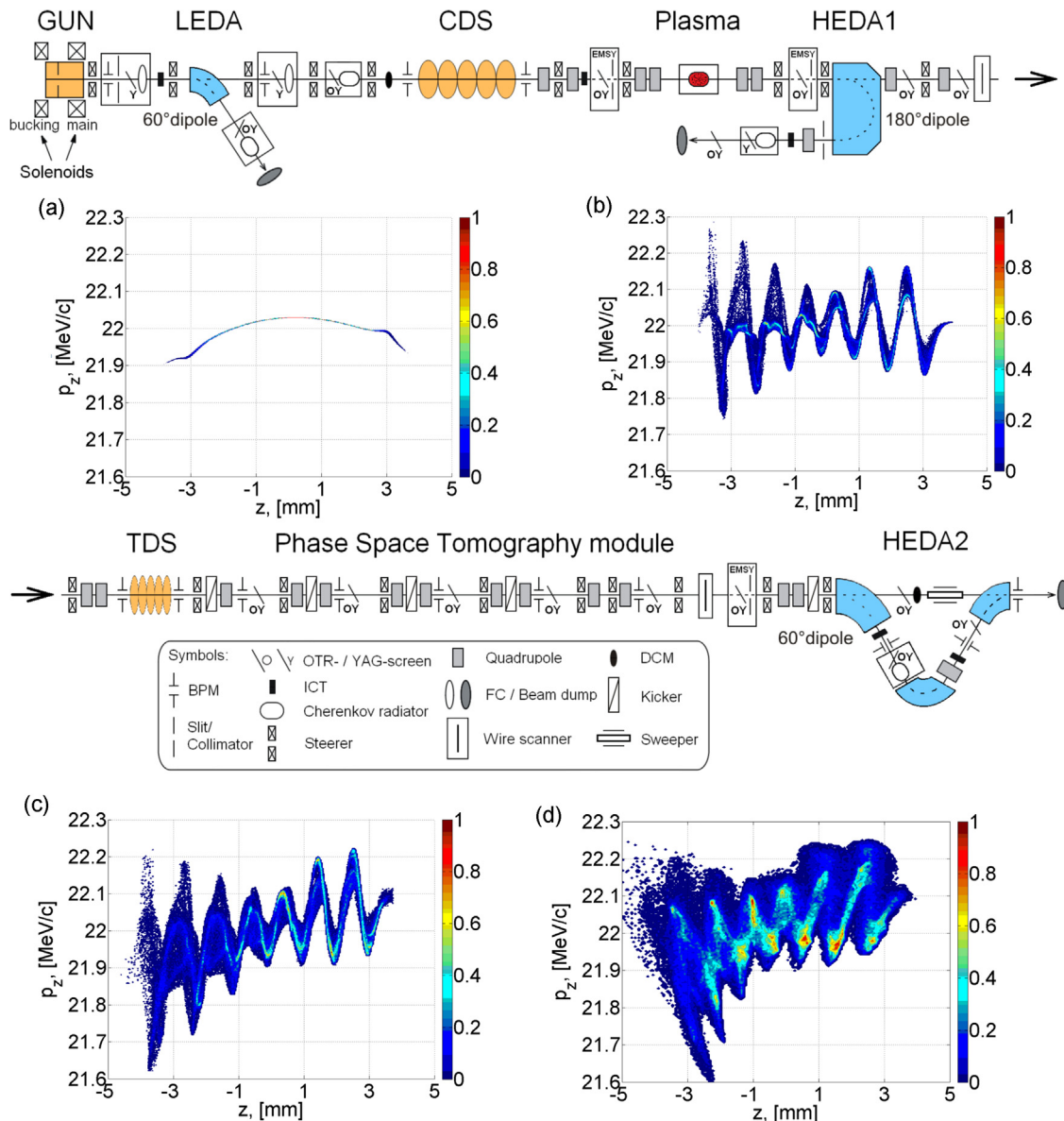

Fig. 1. Block diagram of PITZ beamline and the simulated longitudinal phase space (a) at the plasma cell entrance, (b) after the plasma cell, (c) after TDS, (d) after HEDA2 dipole.
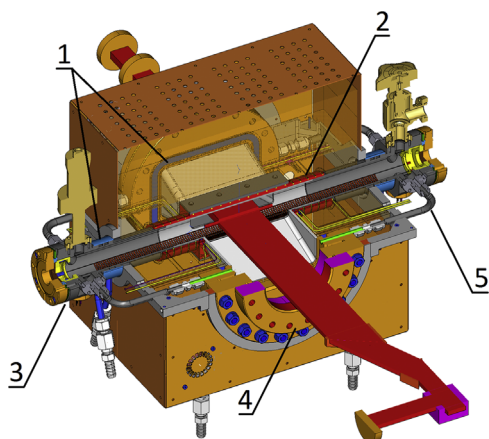
Fig. 2. Design model of the PITZ plasma cell. 1 – cooling sleeve, 2 – heating coil, 3 – electron window, 4 – laser window, 5 – buffer gas distribution pipe. For more details refer to the text.
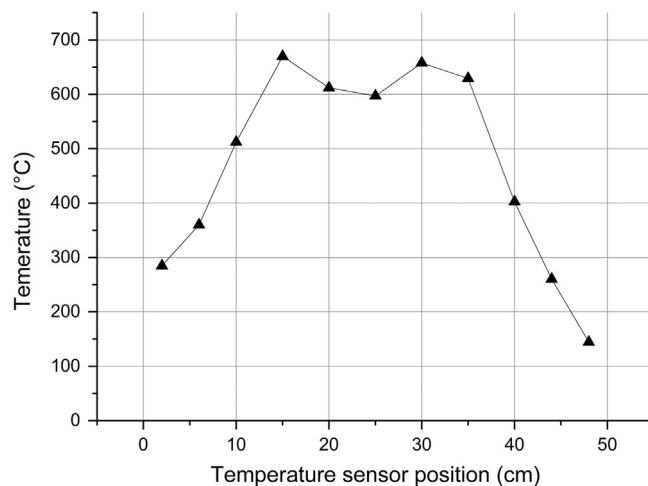

Fig. 3. Temperature distribution inside the plasma cell along the beam pipe, without lithium, measured with a movable temperature sensor. The temperature of the heating element at the center is 720 °C.

coupling into the plasma cell through the orthogonal pipe. Two ionization laser port windows at the ends of the orthogonal pipe are also protected with buffer gas zones. All four gas zones are connected together for pressure equalization. It is possible to control the plasma channel geometry (especially the plasma channel length as well as the plasma density) by means of a shadow mask installed on the ionization port. Another advantage of the cross-shaped design is the feasibility of optical plasma characterization methods done through the side ports.

The plasma cell was manufactured in the mechanical workshop at DESY, Zeuthen site. The device consists of five non-magnetic steel pieces welded together and copper heat conducting parts surrounding the cell core. The surface of the copper part has grooves to house four resistive heating elements: two in the center, above and below the core zone, and two at each side around the beam pipe. The core has to be heated up to 1000 K to achieve the desired lithium vapor density. The temperature distribution across the device and the mechanical stress due to thermal expansion were simulated with the ANSYS software, aiding the design process. The temperature distribution without lithium along the main and orthogonal pipes was measured with a movable temperature sensor and it fits well with the simulation (Fig. 3). The temperature drop in the center zone is attributed to heat loses through the side ports. During operation with lithium the temperature at the core zone equalizes due to the heat pipe mechanism. A metal mesh covers the inner surfaces of both main and orthogonal pipes. Due to the complex plasma cell geometry, the mesh consists of several pieces connected with each other with interlacing wires. Liquid lithium distribution over the mesh and the mesh connections was studied separately with a small oven.

5. Ionization laser

The plasma cell was designed in such a way to accommodate two ionization schemes:

- Field ionization – the orthogonal pipe was designed with cone-shaped side ports taking into account the space needed to utilize a multi-pass ionization scheme.
- Single photon ionization – an UV laser with a wavelength of less than 231 nm is needed for lithium ionization.

It was decided to use a Coherent COMPexPro 201 ArF excimer laser (lasing wavelength 193 nm, up to 400 mJ/pulse) for the single photon ionization scheme. Calculations show [15] that about a few hundred mJ pulse energy laser is needed to achieve about 10^{15} cm^{-3} plasma

density. The laser light travels from the optical lab down to the PITZ tunnel via a specially built laser beamline. The beamline is filled with nitrogen and aimed to be sealed to eliminate absorption of the laser by oxygen. Additional optimization of the laser beamline (better alignment and better sealing of the beamline tube) is needed, as a big portion (about 90%) of the laser pulse energy is lost in the current state.

6. Preparatory experiments

a. Beam focusing into the plasma: Beam matching was done using the ASTRA and MADX [16] codes. First, the electron beam was tracked down to the end of the booster with ASTRA, then, using parameters obtained from ASTRA as input for MADX, proper quadrupole settings for best matching were found. Afterwards the beam was tracked down to the plasma entrance with ASTRA. The quadrupole settings were found for different possible beam scattering angles at the electron windows. To verify these ASTRA simulation results an experiment was conducted where a screen station was mounted at the plasma cell position. The simulation result for the beam matching to achieve a beam with a 40 μm rms radius in the focus is shown in Fig. 4(a). A beam image taken from the screen station with the quadrupole settings obtained from the simulation is shown in Fig. 4(b). The rms beam size is roughly 100 μm. Possible reasons for the discrepancy are a suboptimal beam transport (not ideal alignment of the quadrupoles) in the experiment and low resolution of the screen (estimated at about 50 μm [17]).

b. To study the effect of the electron beam scattering at the electron window foils, ASTRA simulations were conducted: scattering was introduced by increasing the opening angle of the beam at the foil position. It was found that the scattering at the foils can be reduced to acceptable level if the maximum divergence angle due to the beam scattering is less than 0.2 mrad. The simulated horizontal and vertical beam emittances without foils are 0.37 mm mrad and 0.38 mm mrad [18] and no significant change of emittance is expected after passing the foil. Thin polymer films are the favorite material for the electron windows, since they have long radiation lengths (especially polypropylene and polyethylene), therefore they introduce a low amount of scattering and they are strong
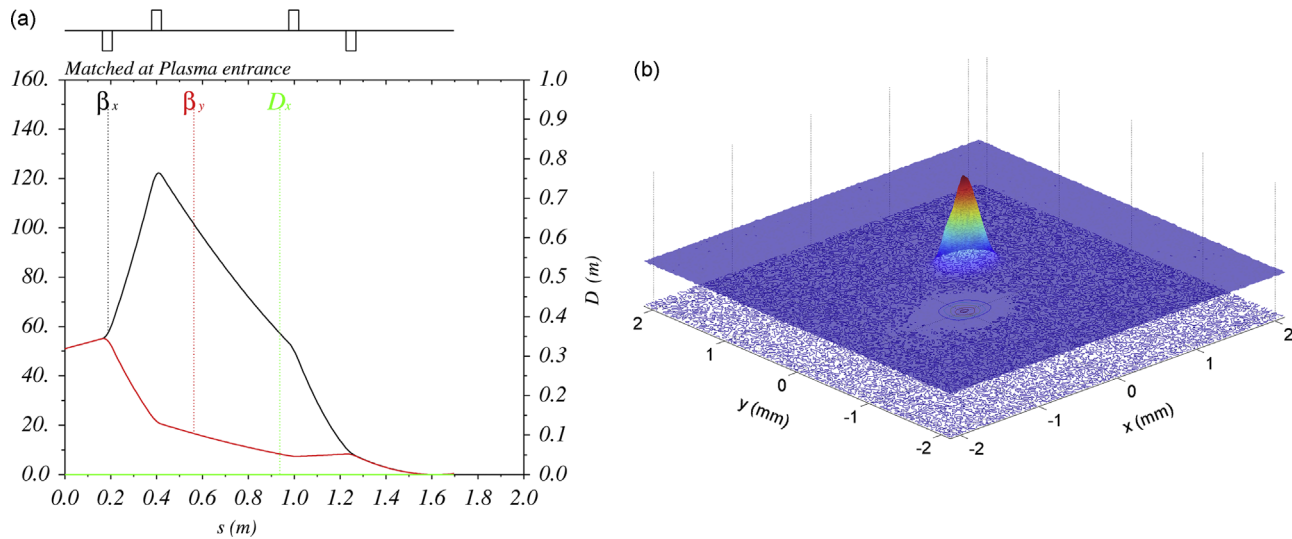
Fig. 4. (a) Simulation: The rms beam size at the entrance of the plasma is 40 μm. (b) Experiment: rms beam size at the entrance of the plasma is about 100 μm.
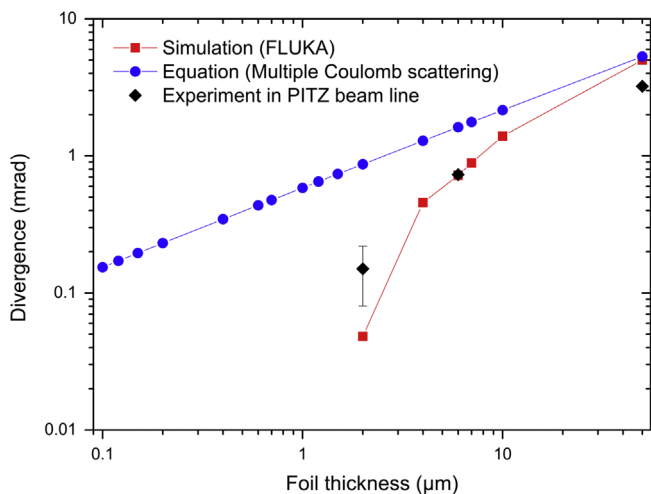

Fig. 5. Electron beam scattering at polymer foils.

enough to withstand the pressure difference between the plasma cell atmosphere and the surroundings, especially during preparation and pumping down (the pressure difference when inserted into the beamline under vacuum is less than 1 mbar). Kapton remains mechanically stable even at high temperatures (up to 400 °C) and is therefore a prime candidate. To estimate the electron beam scattering, different approaches were taken:

- An analytical estimation using multiple Coulomb scattering mechanism [19].
- Scattering simulation with the FLUKA [20] code assuming a transverse Gaussian particle distribution.
- Measurements of the electron scattering in the PITZ beamline.

Fig. 5 shows reasonable agreement between the simulation and the measurement. The analytical estimation fits well for a foil thickness of several tens of μm and more, but breaks down for thinner foils. The reason for this is that the number of scattering processes is reduced so much that the simple statistical approach underlying the equation is not valid anymore. All methods demonstrate an exponential growth of the scattering, and simulation and experiment suggests maximal allowable window thickness of about 3 μm. Amongst others a 2 μm thick Mylar foil

was tested in experiment and showed a scattering angle of 0.15 mrad, which is acceptable.

c. Gas permeation through the electron windows and their mechanical strength are constraining factors for the electron window thickness. If the buffer gas current through the foil exceeds $1 \cdot 10^{-6}$ mbar l/s, stable operation of ion getter pumps and of the RF system in the PITZ beamline is not guaranteed. Literature data on gas permeation through thin foils is contradictory [21–23], therefore several samples of Mylar and Kapton foils with various thicknesses were tested. In these experiments the 2 μm Mylar foil failed the tests and had therefore to be sorted out. A dummy plasma cell was installed into the PITZ beamline to study the stability of the windows during the experiment beforehand. This is a tube terminated with the actual electron windows designated for the experiment and filled with argon gas to nominal working pressure. 8 μm Kapton windows showed acceptable gas load to the PITZ vacuum system and no change of properties after continuous long term operation with an electron beam exceeding nominal power and repetition rate for the experiment. This foil was chosen for the initial experiment despite strong electron scattering, while search for a more suitable material and thickness is ongoing. A 0.9 μm PET film coated with 37.5 nm aluminum on both sides from Astral Technology, currently in test at PITZ is a promising candidate.

7. First run

As a next step in preparation to the self-modulation experiment, the plasma cell was heated up in the lab and the lithium vapor density was measured with the white light absorption method [14]. The measured lithium vapor density was about $4 \cdot 10^{13}$ cm^{-3}, which is much below the target density. This was caused by imperfections in the heat pipe oven, which is described in section below. The ArF ionization laser was coupled through the side port of the plasma cell, and plasma was generated (Fig. 6).The plasma cell was installed into the PITZ beamline and a search for the self-modulation was carried out. Beam transport through the plasma cell was successful; however, the signal to noise ratio at the TDS screens was too poor to make a reliable measurement, so a YAG screen behind the plasma cell was used
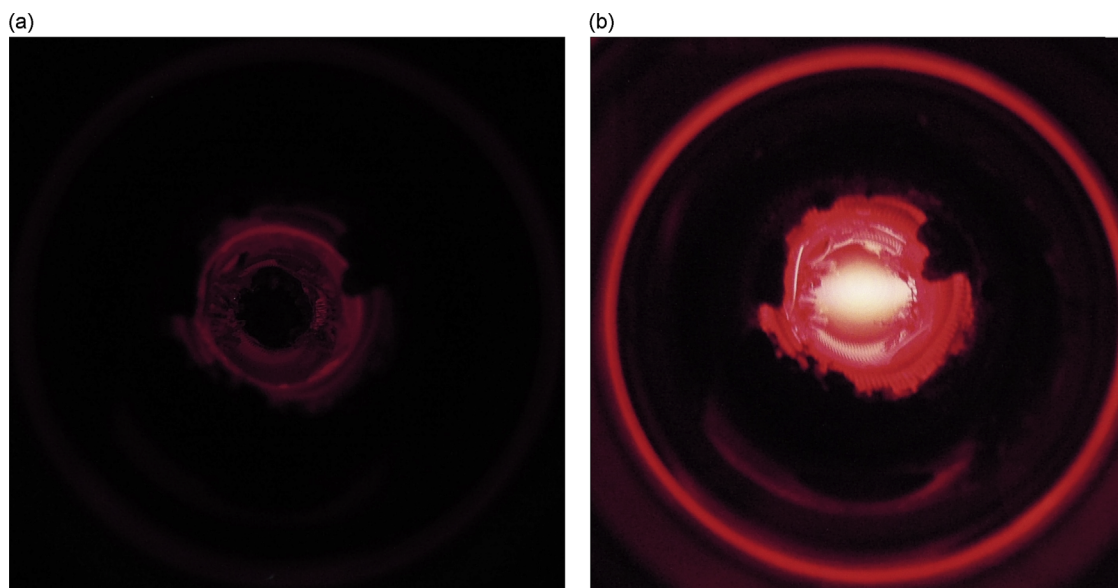
(a)   (b)

Fig. 6. Inside of the plasma cell as seen along the beam pipe. (a) Ionization laser is off – the glowing wire mesh can be seen. (b) Ionization laser is on – coupled in from the side in the image plane. The plasma glow is clearly visible.

for the search of the self-modulation signature. Following parameters were scanned:

- Ionization laser timing with respect to the electron beam.
- Main solenoid current and quadrupoles strengths to find the best beam matching.

No self-modulation was observed and on the sixth day of continuous operation the beam path through the plasma cell was blocked by a ball of lithium condensed at one of the cool ends of the plasma cell heat pipe.

8. Discussion

The first experiment revealed some problems and their possible solutions:

- Lithium condensation in the beam pipe: a possible reason is a wrong metal mesh size. If pores in the mesh are too large, the mesh does not provide enough capillary force. The lithium condensed inside the main pipe, where the mesh is a single piece, which means that the mesh connection, a novel feature of our heat pipe oven is not causing that problem. It is suggested in [24] to use metal meshes with a mesh number (the number of openings per linear inch) in a range between 40 and 300. The mesh which was used for the first experiment had only 26 openings per linear inch. Therefore we will use a denser mesh for the next experiments.
- Low vapor density: if the capillary system of the plasma cell is not 100% effective the lithium circulation is not efficient and a certain amount of lithium will be condensed over time in the cool zones of the plasma cell and therefore will be excluded from the normal circulation. Another possible reason is an insufficient temperature of the core zone: this will be fixed by redesigning the orthogonal pipe shape (constant, small diameter adapted to the beam profile of the ArF ionization laser for less heat loss) and increasing the heater power.
- Low plasma density or strong plasma inhomogeneity: The laser beamline will be adjusted to provide more laser pulse power. This will be accomplished for one part by optimization of the beam transport: simple spherical lenses will be replaced by

cylindrical lenses or mirrors for a better beam profile and less losses. Additionally the beam piping will be improved to minimize the amount of oxygen in the beam path.
- Scattering of the electron beam: the 8 μm thick Kapton foil, which was used in the experiments caused strong scattering, preventing efficient focusing of the electron beam into the plasma. This will be fixed by using a thinner foil: a 0.9 μm PET film coated with 37.5 nm aluminum on both sides has shown sufficient strength, low enough gas permeability and low electron beam scattering and is therefore a prime candidate.

9. Summary

First experiments towards demonstrating the self-modulation of the PITZ electron beam were conducted and the effort is ongoing. Several preparatory experiments were finished where key features of the main experiment were prepared. Firstly, a screen station was installed at the plasma cell position to tune focusing of the electron beam into the plasma channel with a beam size of about 100 μm rms radius demonstrated. Secondly, the scattering of electron beams at thin foils was investigated thoroughly by analytics, simulation and experiment. Necessary conditions were identified and a prime candidate was found. Thirdly, a stress test with a dummy plasma cell was conducted and it was demonstrated that plasma experiments can be conducted in the PITZ beamline without endangering the accelerator. After conclusion of these experiments the plasma cell was put into operation. Plasma was generated in a cross-shaped heat pipe oven for the first time, but no self-modulation instability was observed yet. This was caused by several factors: low gas density, low ionization laser pulse energy and strong electron beam scattering at the window foils. Experience gained in the first run with the plasma cell will be used to improve the experimental setup. A new plasma cell will be designed and manufactured, taking into account the shortfalls of the current design. An in situ plasma diagnostics will be implemented in the setup. Beam matching will be further optimized for the specific electron window type to be used in the next run, which is planned to commence in 2016.

Acknowledgements

References

[1] R. Assmann, et al., Plasma Physics and Controlled Fusion 56 (2014) 084013.
[2] P. Muggli, AWAKE Collaboration, The AWAKE Proton-Driven Plasma Wakefield Experiment at CERN, in: Proceedings of IPAC2015, Richmond, VA, USA, pp. 2502–2505.
[3] A. Caldwell, et al., Nature Physics 5 (2009) 363.
[4] C. Schroeder, et al., Physics Review Letters 107 (2011) 145002.
[5] K.V. Lotov, Instability of long driving beams in plasma wakefield accelerators, in: Proceedings of 6th European Particle Accelerator Conference, Stockholm, 1998, pp. 806–808.
[6] N. Kumar, A. Pukhov, K. Lotov, Physics Review Letters 104 (2010) 255003.
[7] J. Vieira, et al., Physics of Plasmas 19 (2012) 063105.
[8] I. Will, G. Klemz, Optics Express 16 (2008) 14922.
[9] H. Huck et al., First results of commissioning of the PITZ transverse deflecting structure, in: Proceedings of FEL2015 Conference, Daejeon, Korea, 23–28 August, 2015, #MOP039 (2015).
[10] A. Martinez de la Ossa et al., Self-modulation of long electron beams in plasma at PITZ, in: Proceedings of AIP Conference, 1507, 2012, 588.
[11] T. Mehrling, et al., Plasma Physics and Controlled Fusion 56 (2014) 084012.
[12] G. Pathak et al., Simulations study for self-modulation experiment at PITZ, in: Proceedings of 6th International Particle Accelerator Conference, Richmond, VA, USA, paper WEPWA005, 2015, pp. 2496–2498.
[13] K. Flöttmann, ASTRA, DESY. ⟨https://www.desy.de/~mpyflo/⟩.
[14] P. Muggli, et al., IEEE Nuclear and Plasma Sciences Society 27 (3) (1999) 791.
[15] M. Gross, et al., Nuclear Instruments and Methods in Physics Research Section A: Accelerators, Spectrometers, Detectors and Associated Equipment 740 (2014) 74.
[16] MAD-Methodical Accelerator Design. ⟨https://madx.web.cern.ch/madx/⟩.
[17] S. Rimjaem et al., Comparison of Different Radiators Used to Measure the Transverse Characteristics of Low Energy Electron Beams at PITZ DIPAC20112011, Hamburg Germany, pp. 428–430.
[18] M. Khojoyan et al., Beam dynamics studies for particle driven plasma wakefield acceleration experiments at PITZ, in: Proceedings of ICAP2012, Rostock-Warnemünde, Germany, 2015, pp. 236–238.
[19] H. Wiedemann, Particle Accelerator Physics, Springer, Berlin Heidelberg New York (2007), p. 321.
[20] FLUKA Team. ⟨http://www.fluka.org⟩.
[21] S.J. Schowalter, C.B. Connolly, J.M. Doyle, Nuclear Instruments and Methods in Physics Research Section A: Accelerators, Spectrometers, Detectors and Associated Equipment 615 (2010) 267.
[22] H.M. Herring, ChAracterization of Thin Film Polymers Through Dynamic Mechanical Analysis and Permeation, NASA/CR-2003-212422, NAS 1.26:212422.
[23] J.T. Hoggatt, Investigation of the Feasibility of Developing Low Permeability Polymeric Films, NASA-CR-120892, ASG-2-5540.
[24] J.-M. Tournier, M.S. El-Genk, HPTAM, a Two-Dimensional Heat Pipe Transient Analysis Model, Including the Startup From a Frozen State, NASA-CR-199553, NAS 1.26:199553, UNM-ISNPS-4-1995.